Advances in Geo-Energy Research

Vol. 6, No. 5, p. 388-401, 2022

Original article

Criteria and favorable distribution area prediction of Paleogene effective sandstone reservoirs in the Lufeng Sag, Pearl River Mouth Basin

Sa Yu[1], Cheng Wang[2,3], Dongxia Chen[2,3]*, Bowei Guo[2,3], Zhe Cai[2,3], Zhi Xu[2,3]

[1]*Shenzhen Branch of China National Offshore Oil Corporation (CNOOC) Limited, Shenzhen 518054, P. R. China*

[2]*State Key Laboratory of Petroleum Resources and Prospecting, China University of Petroleum, Beijing 102249, P. R. China*

[3]*College of Geosciences, China University of Petroleum, Beijing 102249, P. R. China*

Keywords:
Lufeng Sag
effective reservoir
capillary force ratio
quantitative evaluation
favorable area prediction

Cited as:
Yu, S., Wang, C., Chen, D., Guo, B., Cai, Z., Xu, Z. Criteria and favorable distribution area prediction of Paleogene effective sandstone reservoirs in the Lufeng Sag, Pearl River Mouth Basin. Advances in Geo-Energy Research, 2022, 6(5): 388-401.
https://doi.org/10.46690/ager.2022.05.04

Abstract:
As the focus of conventional oil and gas exploration is changing from shallow to deep layers, the identification of deep effective reservoirs is crucial to exploration and development. In this paper, based on the geological anatomy of oil and gas reservoirs, a new discriminatory criterion and evaluation method for effective reservoirs is proposed in combination with the analysis of reservoir formation dynamics mechanism. The results show that the hydrocarbon properties of the reservoir vary with the ratio of the capillary force between the sandstone reservoir and its surrounding rock. The effective reservoir is discriminated and the reservoir quality is evaluated based on the capillary force and depth of the surrounding media and the sandstone reservoir for adjacent plates. When the capillary force ratio is greater than 0.6, fewer effective reservoirs are developed. The effective reservoir is determined by the capillary force ratio of the sandstone reservoir and the surrounding rock medium to mechanically explain the geological phenomenon that low-porosity reservoirs can also accumulate hydrocarbons. Our findings have significant guiding value for Paleogene oil and gas exploration in the Zhu I depression of Pearl River Mouth Basin.

1. Introduction

With the focus of oil and gas exploration gradually shifting to deeper layers, deeper oil and gas resources are also receiving more and more attention from oil workers (Athens and Caers, 2019). Deep geological exploration has high uncertainty and considerable exploration risk, and obtaining a reliable and simple method to determine the effective reservoir in deep strata is an important issue directly related to the exploration process (Mohaghegh 2014; Wang et al., 2019; He et al., 2020; Okunuwadje et al., 2020; Barach et al., 2021; Tang et al., 2022). The development and distribution of different types of high-quality reservoirs are controlled by the combination of tectonic, stratigraphic, petrographic, fluid and time factors, among which the evaluation of effective reservoirs is a popular issue in deep oil and gas exploration (Huang et al., 2020; Zeng et al., 2020). Oil and gas mainly accumulate in high-porosity and high-permeability reservoirs in the shallow layer. And deeper in the basin, hydrocarbons can accumulate in low-porosity, low-permeability reservoirs that were previously thought to be ineffective (Wang et al., 2003; Ehrenberg and Nadeau, 2005). Regarding the identification of effective reservoirs, some scholars define reservoirs that can be developed under the current technical conditions as effective reservoirs based on reservoir tests and production data (Zhou et al., 2022); other scholars have considered these reservoirs as ones capable of storing and percolating fluids and producing industrially valuable volumes of liquids (hydrocarbons or a

Yandy Scientific Press

*Corresponding author.
E-mail address: yusa@cnooc.com.cn (S. Yu); w396524765@163.com (C. Wang); chendx@cup.edu.cn (D. Chen); guobowei@foxmail.com (B. Guo); 937884783@qq.com (Z. Cai); 2019215045@student.cup.edu.cn (Z. Xu).

Received April 29, 2022; revised May 25, 2022; accepted June 19, 2022; available online June 26, 2022.

mixture of hydrocarbons and water), which can be extracted by existing technologies (Huang et al., 2021). It has also been argued that, in the general context of low porosity and low permeability, reservoirs with relatively high porosity and permeability are considered as effective reservoirs (Wang et al., 2014; Zhu et al., 2020). Previous discriminations of effective reservoirs were mainly based on the physical property data of cores and logging data that determine the lower limit of the physical properties of effective reservoirs (Sun et al., 2019; Huang et al., 2020; Li et al., 2022). This approach is suitable under the condition of abundant data, while there may be great uncertainty in case there is a lack of data. Importantly, most of the values obtained by this method are the present-day lower critical limits of the reservoir, but not the lower physical limits of the reservoir at the time of formation. Besides, the reservoir formation process is not considered, and the value is often fixed at a certain level in a specific area, which is not consistent with reality (Purcell, 1949; Wu et al., 2020).

In recent years, the exploration and development practices have proved that the lower critical physical limits of effective reservoirs vary with the burial depth. For example, in the cretaceous sandstone reservoirs of western Alberta Basin, Kuqa depression of Tarim, Jiyang depression of Bohai Bay Basin, and Nanpu depression, the lower limits of the critical physical properties of reservoirs decrease with burial depth (Masters, 1979; Huo et al., 2014; Jiang et al., 2014, 2015). In the Lufeng Sag of Pearl River Mouth Basin, Paleogene effective reservoirs developed under 4,000 m, but due to certain geological phenomena, effective reservoirs did not develop under some shallow burial layers (Wang et al., 2022). This indicates that burial depth is not the decisive factor restricting the development of effective reservoirs. The analysis of pore permeability data in the Lufeng Sag of Zhu I Depression in the Pearl River Mouth Basin shows that oil and gas can be charged into the reservoir only when the physical properties of the reservoir under a certain burial depth exceed a given critical value. However, this is not a fixed value but it shows a decreasing trend with the increase in burial depth, indicating that the effective reservoir criterion changes dynamically with depth. It is difficult to rely on physical statistics alone to identify effective reservoirs for specific exploration and development needs, and the underlying causes of this phenomenon cannot be explained mechanistically. Therefore, it is urgent to construct a new method that is suitable for effective reservoir discrimination in the Lufeng Sag.

Based on analyzing the dynamic mechanism of reservoir formation and the difference in capillary force between a sandstone reservoir and the surrounding rock medium, this paper reveals the variation law of the lower limit of effective reservoir physical properties with burial depth. It is established that the more obvious the pore throat relationship between sandstone reservoir and the surrounding rock medium, the greater the difference in capillary force, and the more favorable it is for the accumulation of oil and gas and effective reservoir formation. The ratio of capillary force between sandstone reservoir and the surrounding rock medium and the relationship between reservoir oil-gas-water distribution are quantitatively analyzed, so as to establish effective reservoir discrimination and quantitative evaluation standards. This strategy is used to optimize the favorable areas for oil and gas exploration in the deep Lufeng Sag of Zhu I depression.

2. Geological setting

2.1 Location and geological setting

The Pearl River Mouth Basin is one of the most important oil and gas production areas in the South China Sea (Tian, 2022). The Lufeng Sag is located in the northern part of the Zhu I depression, with an area of 7,760 km^2. From north to south, it is divided into Northern Uplift Zone, Northern Depression Zone, Central Uplift Zone, Middle British Depression Zone, Southern Uplift Zone, and Southern Depression Zone (Fig. 1). The Cenozoic tectonic evolution of the Pearl River Mouth basin includes three stages: rifting, depression and rapid subsidence (Wang et al., 2019). The Wenchang Formation and Enping Formation were mainly deposited in the lacustrine rift stage during the Eocene.

The sediment thickness of the Enping and Wenchang Formations exceeds 4,500 m (Ge et al., 2020), of which the former can be subdivided into four subsections, and the latter can be subdivided into six subsections. These two formations experienced a complete set of sedimentary cycles. In the initial period, deposition in the lake basin mainly occurred by the braided river delta sand body; in the peak period, it occurred by the semi-deep lake-deep lake phase mudstone; in the shrinking period, deposition continued by the coastal shallow lake sand mudstone interlayer. The lake basin of Wenchang Formation was small in the initial sedimentary period. Controlled by the Hui-lu low uplift, Lufeng low uplift and Dong-sha uplift, a braided river delta depositional system developed. With the intensification of fault activity, the lake basin deepened, and a large area of deep lacustrine sedimentary system developed in the fourth member of Wenchang Formation. In the late depositional stage, the area of deep lacustrine facies decreased and the braided river delta further developed.

2.2 Research technology route

In this study, the geological background of the study area is fully investigated, and the characteristics of the high-quality reservoir are clarified using analytical and laboratory data, such as rock thin sections, scanning electron microscopy, reservoir properties, and drilling and logging data. The capillary force differences around reservoirs are calculated by combining geological statistics and numerical simulation, and the quantitative criterion of a reservoir is established. The effective reservoir is discriminated and reservoir quality is evaluated based on the cross chart of capillary force and the depth of sandstone reservoir and the surrounding rock medium. It is found that the higher the capillary force ratio, the better the reservoir quality. The capillary force ratio between sandstone reservoir and the surrounding rock is normalized, and the normalized value is defined as the potential difference index P_I. The critical conditions for the development of effective reservoirs are clarified by using the potential difference index P_I, and then the favorable areas in the study area are predicted.

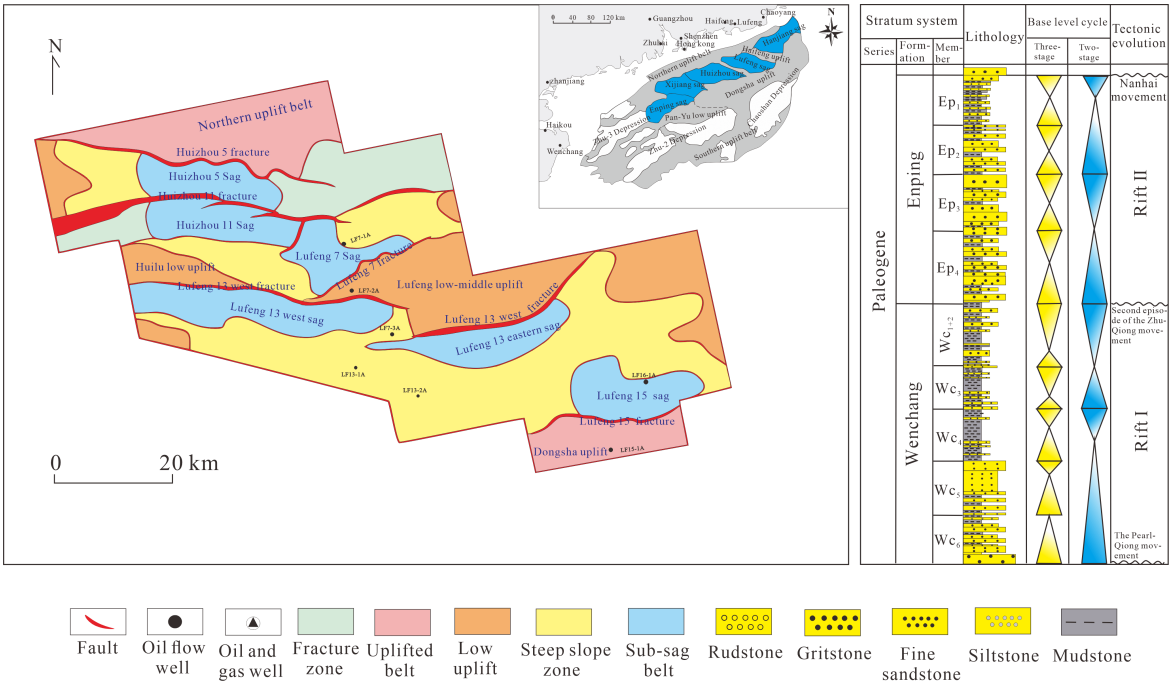

Fig. 1. Structural position and stratigraphic histogram of Lufeng Sag.

3. Methods and results

3.1 Effective reservoir identification criteria and evaluation principles

(1) Concept of effective reservoir

Effective reservoir is defined in this paper as reservoir rock that can collect hydrocarbons and form hydrocarbon reservoirs under certain geological conditions. The oil-bearing property of an effective reservoir is controlled by the matching relationship between the driving forces of oil-gas accumulation, and oil and gas always accumulates in the low-potential area (Wang et al., 2003). Buoyancy, formation pressure, hydrodynamic force and capillary force together determine the magnitude of the fluid potential. However, the four fluid potentials do not play the same role in the transport of hydrocarbons during reservoir formation (Hubbert, 1940, 1953). The historical data show that there is a bottom line for hydrocarbon accumulation in sedimentary basins, which is the maximum depth at which hydrocarbons are controlled by buoyancy; under this line, hydrocarbon migration is not affected by buoyancy (Pang et al., 2013). The development of overpressure in a deep basin has an important influence on hydrocarbon migration and accumulation, while the formation pressure hardly impacts hydrocarbon migration and accumulation under normal pressure conditions. Formation water is also in the hydrostatic state under normal pressure conditions. Besides, the hydrodynamic effect is not obvious in the hydrostatic state. In the deep formation environment, compaction results in the rapid reduction of sandstone pores, while the compaction effect of mudstone pores is not as marked. In this way, a large capillary force difference is formed between them, which has a great influence on oil and gas migration (Wang et al., 2020), as it is the driving force of hydrocarbon migration and accumulation in conventional deep basins. Effective reservoirs form under the action of capillary force difference (Fig. 2).

(2) Genesis mechanism

Pang et al. (2013) simulated the migration of oil and gas between sandstone and the surrounding rock media through physical experiments, and explained the reservoir effectiveness. They argue that the accumulation of hydrocarbons in the reservoir is not determined by the absolute porosity size of the sandstone, but depends on the relative pore throat radius of the sandstone and the surrounding media (Pang et al., 2013). Only when the pore throat radius of sandstone is more than 2 times of that of the surrounding rock, are oil and gas likely to accumulate in sandstone. Moreover, and the ratio of oil saturation to pore throat radius of sand mudstone shows a positive correlation (Pang et al., 2012).

The experimental results show that whether oil and gas can accumulate in sandstone reservoirs is influenced by the ratio of pore throat radius between the reservoir and its surrounding rock; the greater the porosity difference, the larger the difference in capillary force. Under the action of capillary force difference, oil and gas migrate from sandstone with smaller pore throat radius to sandstone with larger pore throat radius (Berg, 1975). The difference in capillary force between the inside and outside of a reservoir is the basic driving force of hydrocarbon accumulation and is an important basis for discriminating effective reservoirs. The capillary force of oil and gas in the pore structure of rock is mainly related to the contact angle of the multiphase fluid present, the radius of pore throat in the rock medium, and the interfacial tension of fluid, such as:

$$P = \frac{2\sigma\cos\theta}{a} \tag{1}$$

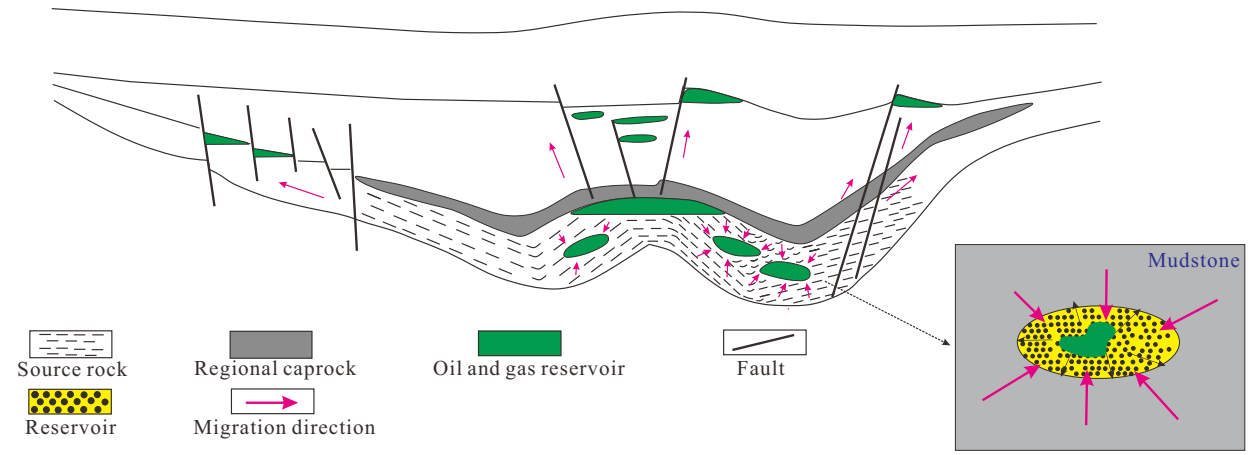

Fig. 2. Conceptual model of an effective reservoir.

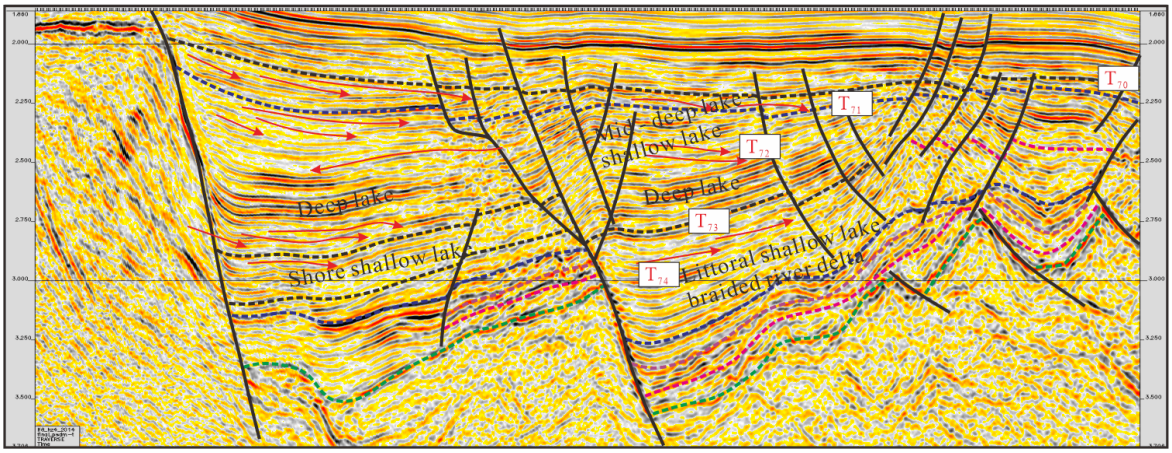

Fig. 3. Typical seismic facies profiles in the Lufeng Sag.

where P represents the capillary pressure, Pa; θ represents the angle between the two-phase interface and the horizontal plane, °; σ represents the interfacial tension, N/m; a represents the pore throat radius, μm.

Interfacial tension is generally influenced by the fluid properties and temperature. The gas-water interfacial tension is generally greater than the oil-water interfacial tension, and the oil-gas-water interfacial tension decreases with increasing temperature. Underground rocks are generally hydrophilic, and the wetting angle θ between hydrocarbon fluids and water mostly ranges between 0-30° (England et al., 1987). Pore throat radius is an important parameter to characterize pore structure and is a key indicator of reservoir quality. The capillary force in reservoirs is generally proportional to the interfacial tension σ, inversely proportional to the wetting angle θ, and inversely proportional to the pore throat radius a. The interfacial tension σ and wetting angle θ remain constant when hydrocarbon migrates to adjacent pore structures, and the capillary force is mainly controlled by the difference in pore throat radius between porous media. The capillary force ratio of the surrounding rock medium to the reservoir is only related to the relative size of the pore throat radius of sandstone and surrounding mudstone. Therefore, the capillary force ratio between the surrounding rock medium and the reservoir can be characterized as:

$$I = \frac{\frac{2\sigma\cos\theta}{r}}{\frac{2\sigma\cos\theta}{R}} = \frac{R}{r} \tag{2}$$

where I represents the ratio of capillary force between the surrounding rock medium and the reservoir, dimensionless; R represents the pore throat radius of sandstone, μm; r represents the radius of pore throat in mudstone medium, μm.

The research data show that the larger the difference between the pore throat radius of mudstone and that of the reservoir, the larger the ratio of capillary force between them, and the more favorable this is to hydrocarbon accumulation.

(3) Effective reservoir identification and evaluation methods

Geological statistical methods are commonly employed to calculate the differences in capillary force in and around a reservoir, so as to establish the quantitative discrimination standard of that reservoir. In this paper, the relationship between the sandstone reservoir porosity and the median pore throat radius is established. Then, the relationship between pore throat radius and the buried depth of mudstone in the study area is fitted. On the basis of the relationship between

Table 1. Potential difference index and reservoir classification of Paleogene reservoirs in the Lufeng Sag.

Formation	Logging interpretation	$0 \le P_I < 0.3$	$0.3 \le P_I < 0.7$	$0.7 \le P_I < 1$	$P_I \ge 1$
Enping	Water layer (%)	72	28	0	0
	Oil-bearing water layer (%)	29	65	6	0
	Oil-water layer (%)	50	50	0	0
	Oil layer (%)	66	31	3	0
	Dry layer (%)	0	0	33	67
Wenchang	Water layer (%)	20	78	2	0
	Oil-bearing water layer (%)	30	68	2	0
	Oil-water layer (%)	25	25	50	0

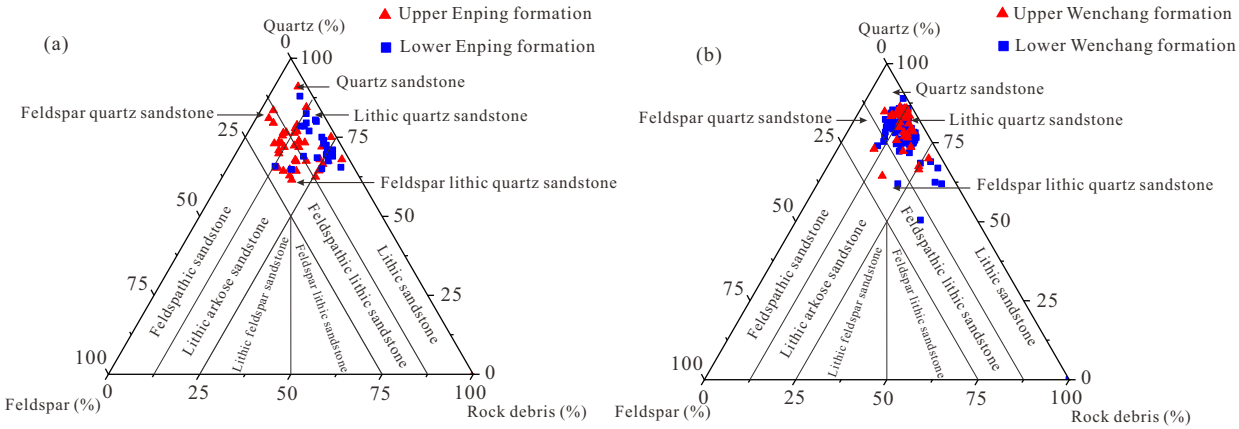

Fig. 4. Statistical map of the reservoir rock types of (a) Enping Formation and (b) Wenchang Formation in the Lufeng Sag.

the porosity and pore throat radius of sand-mudstone, the capillary force distribution characteristics of oil layer, oil-water layer, water layer and dry layer in sandstone reservoir and its surrounding rock (mainly mudstone) are calculated (Eq. (2)). Then, the ratio of capillary force between sandstone reservoir and surrounding rock is normalized to obtain the potential difference index P_I (Eq. (5)). It is found that there is a good correspondence between the development of Paleogene effective reservoirs and the potential index P_I in the Lufeng Sag (Table 1). Effective reservoirs are generally developed when P_I is less than 0.7. As the potential index P_I increases further, a dry layer begins to develop. Meanwhile, when P_I is greater than 1, mainly a dry layer will result (ineffective reservoirs).

3.2 Reservoir characteristics of the Lufeng Sag

(1) Sedimentary system

Based on the comprehensive analysis of cores, well logs and seismic data, in general, five sedimentary systems are developed in the Lufeng depression, including braided river delta, fan delta, shallow lake, deep lake, and lakebed fan (Fig. 4). Braided river delta is an important sedimentary system in the lake basin, which mainly forms in the gentle slope zone along the long axis of the lake basin because of the oil-gas supply system of Lufeng East low uplift and Hui-Lu low uplift. In the seismic profile, braided river deltas generally correspond to oblique and S-shaped seismic facies. The fan delta developed at the edge of hot basin with steep terrain and dry climate. The detrital material entered the sedimentary area quickly from the hydrocarbon area, and had a fast deposition rate. The fan delta deposition mainly occurred near the boundary fault of the 6th member of Wenchang Formation in the initial stage, and the 5th member of Wenchang Formation in the early stage of intense rift. The shore and shallow lake subfacies developed in each sequence of the Enping Formation, which are subparallel wave-like or uncollagenous seismic facies in the seismic profile, with medium-weak amplitude and medium-low continuity. Gray mudstone interbedded with thin argillaceous siltstones developed in each sequence of the Enping Formation and Wenchang Formation. The deep lacustrine and semi-deep lacustrine subfacies are anoxic reducing environments with weak sedimentary hydrodynamics. The seismic profile of deep lake sediments shows that the seismic facies is a parallel sheet reflection with strong amplitude and high continuity, which represents the sedimentary environment with relatively stable energy. These are mainly dark gray and black gray mudstone, which also comprise the main source rock system in the Lufeng Sag. The main subfacies developed in the Wenchang Formation are deep lacustrine and semi-deep lacustrine. The lakebed fan mostly developed in the strong rifting stage of

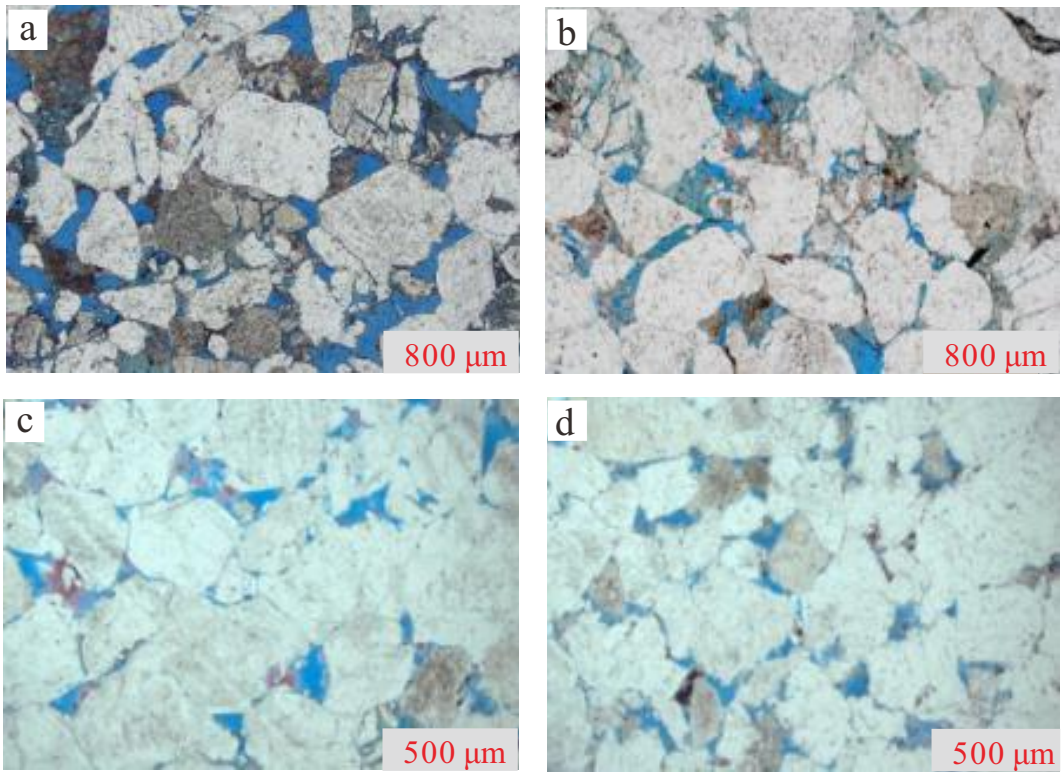

Fig. 5. Rock characteristics of Paleogene reservoirs in the Lufeng Sag: (a) LF8-1A, 3,096 m, Enping Formation, coarse sandy giant sandstone, medium-good sorting, sub-rounded, quartz 77.5%, miscellaneous base 1%, clay minerals 5%, (b) LF8-1A, 3,322 m, Enping Formation, coarse sandy giant sandstone, medium-good sorting, subrounded, quartz 83.5%, miscellaneous base 6%, clay minerals 4.5%, (c) LF14-4-1A, 4,156.76 m, Wenchang Formation, coarse sandstone, medium-good sorting, subrounded-subangular, quartz 87.5%, miscellaneous base 2%, clay minerals 5%, (d) LF14-4-1A, 4,168.95 m, Wenchang Formation, medium-coarse sandstone, medium-good sorting, subrounded-subangular, quartz 83%, miscellaneous base 1%, clay minerals 7%.

the basin, was wrapped in deeper lacustrine rocks, and shows a low amplitude mound-type seismic phase in the seismic profile.

(2) Rock type

The results of rock thin section identification for sandstone reservoirs in the Lufeng Sag indicate that the lithology of the Paleogene Epping Formation is dominated by feldspathic quartz sandstone, accounting for 46.16% (Fig. 4(a)), followed by feldspathic quartz sandstone (31.44%), and rocky quartz sandstone (12.26%). On the other hand, the Wenchang Formation reservoir is dominated by feldspathic quartz sandstone, accounting for 62.40% (Fig. 4(b)), followed by feldspathic quartz sandstone (26.40%), and feldspathic quartz sandstone (7.20%). The comparative analysis shows that the Wenchang Formation is mainly lithic quartz sandstone, while the Enping Formation is less lithic quartz sandstone, but with an increased content of feldspar lithic quartz sandstone.

(3) Rock structures

The grain size of rock has great influence on the reservoir quality. The statistical analysis of thin sections reveals that the grain size of sandstone reservoirs varies greatly. The Wenchang Formation is mainly dominated by coarse sandstone and medium sandstone, occupying 23.36% and 27.31%, respectively. These are followed by fine sandstone and unequal grained sandstone, which take up 26.97% and 15.69%. The Enping Formation is mainly dominated by fine sandstone, accounting for 33.16%, followed by coarse sandstone, medium sandstone and unequal grained sandstone, accounting for 23.13%, 18.96% and 19.36%, respectively. It also contains small amounts of siltstone, giant sandstone and conglomerate reservoirs. Reservoirs with good sorting characteristics have a large and evenly distributed pore space and few fillers in the pores; conversely, poorly sorted reservoirs have an uneven distribution of particle size, with small particles occupying part of the pore space and blocking the pores and roaring channels, which in turn reduces the reservoir porosity and permeability. The sorting degree of Paleogene reservoir sandstone particles in the study area is mainly poor to medium (Fig. 5). Moderately sorted sandstones of the Wenchang Formation and Enping Formation account for about 47.06% and 41.47%, respectively. The sorting degree of Wenchang Formation is higher than that of Enping Formation. The better the roundness of rock particles, the greater the friction force in the process of handling, and the longer the distance of handling. A sandstone reservoir with better roundness has wider pore throat and better connectivity, which yields better reservoir physical properties.

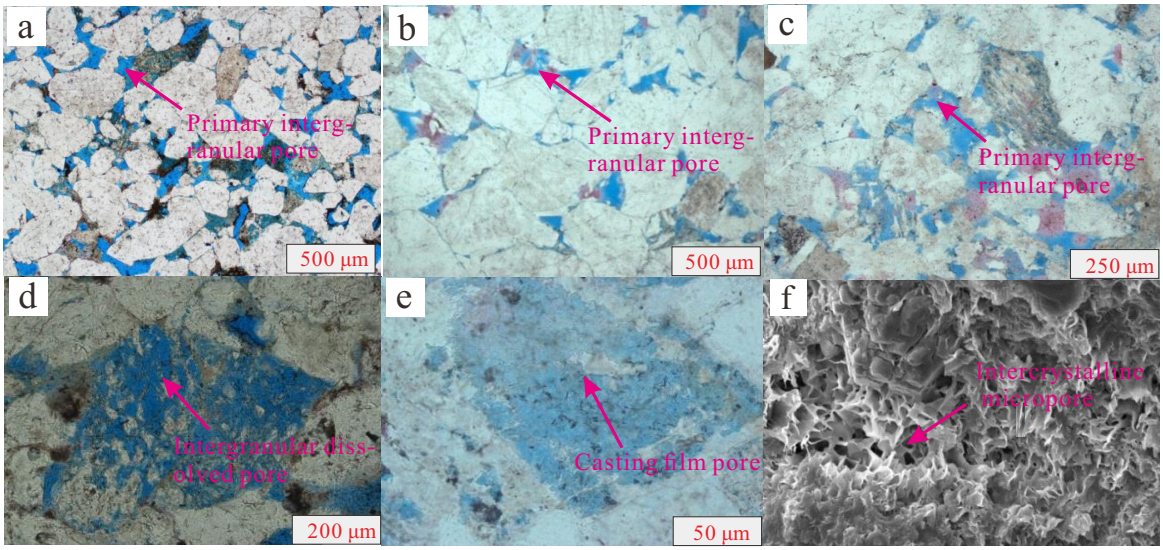

Fig. 6. Microscopic images of the main pore types of Paleogene reservoirs in the Lufeng Sag: (a) LF8-1A, 3,580 m, Enping Formation, particle point-line contact, primary intergranular pore development, plane-polarized light, (b) L14-4-1A, 4,156.76 m, Wenchang Formation, particle point-line contact, primary intergranular pore development, plane-polarized light, (c) L14-4-1A, 4,168.756 m, Wenchang Formation, particle point-line contact, primary intergranular pore development, plane-polarized light, (d) LF14-4-2A, 4,080.5 m, Wenchang Formation, dissolution of debris particles and development of dissolved pores, plane-polarized light, (e) LF14-4-1A, 4,172.71 m, Wenchang Formation, dissolution of feldspar particles to form mold holes, plane-polarized light, (f) LF14-4-1A, 4,099 m, Wenchang Formation, dissolution of feldspar particles to form intragranular dissolved pores, scanning electron microscopy (SEM).

On the contrary, sandstone reservoirs with poor rounding are also poorly sorted; the pore structure is complex, with unequal space size and uneven distribution, with some of the particle angles even blocking or cutting off the throat, reducing the reservoir physical properties. The sandstone grains of Paleogene reservoirs in the study area differ greatly in the rounding degree. The reservoir of Enping Formation is mainly subrounded (Figs. 5(a) and 5(b)), accounting for 49.21%, followed by subrounded-subangular (21.71%). The Wenchang Formation reservoir is mainly subcircular-subangular (Figs. 5(c) and 5(d)), occupying 35.68%, followed by subangular, sub-angular and sub-round, occupying 22.56%, 24.23% and 17.53%, respectively.

(4) Pore type

Through casting thin sections and performing scanning electron microscopy, it is established that primary pores are the main type of pores in the Lufeng Sag, followed by secondary pores. In the SEM images, the primary pores are polygonal or irregular, and the contact between pores and particles is relatively straight without obvious harbor erosion (Figs. 6(a)-6(c)). The secondary pores are mainly intragranular pores and cast film pores formed by the dissolution of unstable minerals such as feldspar and debris (Fig. 6(e)), and intergranular micropores formed by the partial dissolution of clay minerals (Fig. 6(f)). The statistics show that the primary pores of Enping Formation account for a higher percentage of 85%, while the intragranular solution pores, intergranular pores and cast film pores account for 5%, 3% and 2%, respectively. The Wenchang Formation is adjacent to the main source rock, and organic acid corrosion leads to an increase in the secondary pores. The proportion of primary pores is decreased to 73%, while the proportion of dissolved pores, intergranular pores and cast pores account for 10%, 4% and 13%, respectively. Therefore, primary pores in the study area constitute the main reservoir space.

(5) Physical properties

According to the statistics on the physical properties of the Lufeng Sag, the porosity of Wenchang Formation is between 4% and 20%, mainly between 8% and 16%. The permeability ranges from 0.1 to 10,000 mD, and it is mainly distributed between 1-100 mD. The reservoir porosity of the Enping Formation is between 4% and 20%, mainly between 8% and 16%. Its permeability is in the range of 0.1-10,000 mD, mainly in the range of 1-100 mD. The porosity of Enping Formation is 12%-16% higher than that of Wenchang Formation, and the permeability of Enping Formation is 10-100 mD higher than that of Wenchang Formation (Fig. 7). Therefore, the physical properties of Enping Formation are superior to those of Wenchang Formation.

4. Discussion

4.1 Prediction and examination of reservoir favorable zone in the Lufeng Sag

(1) Discriminant criterion and evaluation of reservoirs in the Lufeng Sag

The relationship between sandstone porosity and sandstone pore throat radius was established by the statistical analysis of piezometric experimental data of the sandstone samples from the Lufeng Sag (Fig. 8). The correlation between porosity and

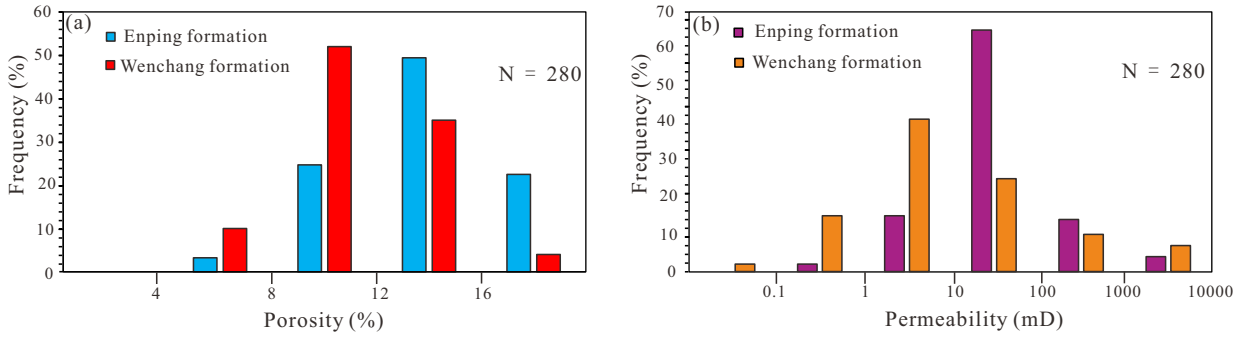

Fig. 7. Distribution map of reservoir (a) porosity and (b) permeability in the Lufeng Sag.

the pore throat radius of sandstone pore throats in the study area is favorable, therefore, we propose to use this model to find the pore throat radius of sandstone reservoirs in the study area, such as:

$$R = 0.0205e^{0.2376\phi} \tag{3}$$

where ϕ represents sandstone porosity, %.

Next, the relationship between buried depth and pore-throat radius is used to simulate the pore-throat radius of mudstone in the study area:

$$r = 6259.1H^{-1.6542} \tag{4}$$

where H represents depth, m.

Approximating the pore throat radius of the mudstone at the same reservoir depth as the pore throat radius of the mudstone surrounding the reservoir, and then the ratio of capillary force difference between reservoirs with different oil-bearing grades in the study area is obtained by using the ratio of pore throat radius (Fig. 9). The demarcation line (solid line on the left) between effective reservoir and ineffective reservoir can be seen in the capillary force difference chart, and this line is taken as the critical condition for distinguishing effective reservoirs. The threshold value of the capillary force difference between the surrounding rock and the reservoir must be satisfied, that is, for an effective reservoir, it needs to be greater than the capillary force ratio at the same depth. Under the condition of a certain burial depth, the porosity and permeability of the reservoir have certain ranges, and there is a maximum value under this burial condition. Therefore, the maximum capillary force ratio can be determined between the sandstone reservoir and the surrounding rock. According to the distribution range of the capillary force ratio of effective reservoirs in the Lufeng Sag, the maximum boundary under different burial depths can be determined (solid line on the right). The trend line of the maximum capillary force ratio increases first and then decreases, while the critical value of the capillary force ratio corresponding to the effective reservoir shows a trend of gradual increase. According to the variation rule of the intersection plate, the maximum value of the capillary force ratio at a burial depth reaching about 5,800 m and the minimum value of the capillary force ratio required for hydrocarbon formation intersect at a certain point, which indicates that the maximum capillary force ratio for hydrocarbon formation at that depth has reached the minimum capillary force ratio for hydrocarbon formation. As the burial depth continues to increase, the maximum capillary force ratio between the surrounding rock and the reservoir will be less than the minimum capillary force required for oil and gas accumulation; therefore, oil and gas cannot accumulate in the reservoir.

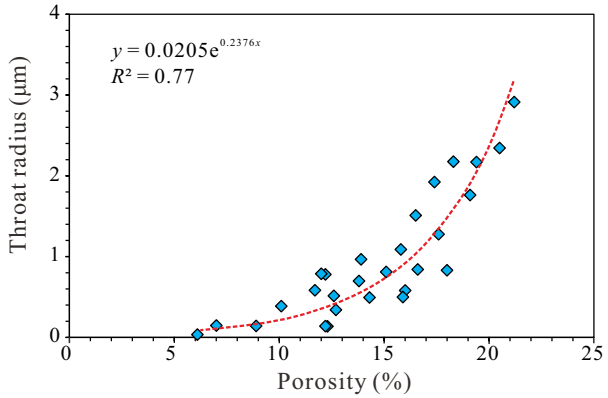

Fig. 8. Relationship between the porosity and pore radius of sandstone in the Lufeng Sag.

For an underground uniform-depth reservoir, the higher the ratio of capillary force between the surrounding rock and sandstone, the better the reservoir quality. Accordingly, the potential difference index P_I is established to quantitatively evaluate the reservoir quality. We assume that a, b and x are data points of the reservoir under the same burial depth, where a represents the critical point of the capillary force ratio of the effective reservoir under this burial depth, x is any point under this burial depth, and b represents the maximum point of the capillary force ratio of the effective reservoir. Then, the potential difference index P_I of any x depth can be expressed as follows:

$$P_I = 1 - \frac{P_x - P_a}{P_b - P_a} \tag{5}$$

where P_I represents the potential difference index, dimensionless; P_x represents the ratio of mudstone capillary force to sandstone capillary force at point x, dimensionless; P_a represents the ratio of mudstone capillary force to sandstone capillary force at point a, dimensionless; P_b represents the ratio of mudstone capillary force to sandstone capillary force

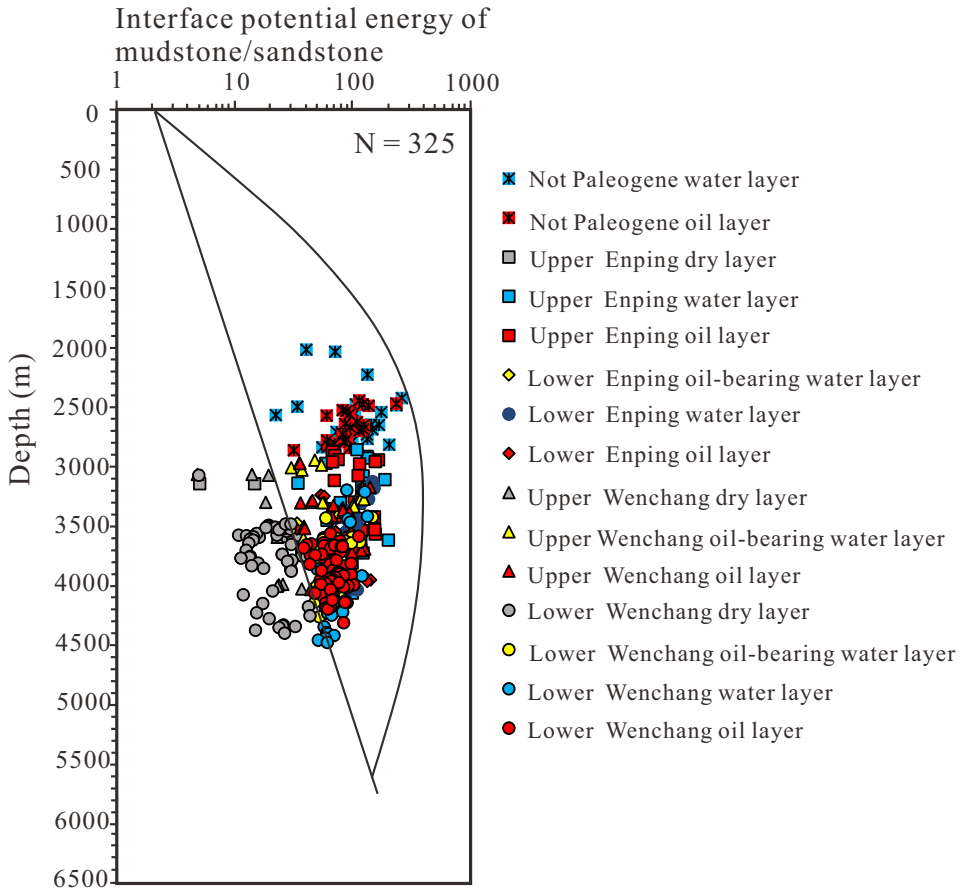

Fig. 9. Capillary force difference diagram of reservoirs in the Lufeng Sag.

at point *b*, dimensionless.

The potential difference index P_I is a standardized concept with values ranging from 0 to 1. Then, the relationship between the potential difference index P_I and oil saturation is established, and the oil saturation has the critical point of maximum capillary force ratio. The oil-bearing saturation of the Enping Formation is high in the reservoir when the P_I is less than 0.5, and *a* dry layer begins to develop above P_I greater than 0.5 (Fig. 10(a)). When the oil saturation of the Wenchang Formation is less than 0.6, the reservoir oil content is high, and when the P_I is greater than 0.6, the dry layer also begins to develop (Fig. 10(b)). Thus, the relationship between oil saturation and potential index P_I can indicate the distribution of oil and gas in the target layer in the study area.

(2) Prediction of favorable reservoir area in the Lufeng Sag

The porosity distribution of Lufeng Sag has a good correspondence with the change of sedimentary phase zone. In the lower Wenchang Formation, the porosity of southern Lufeng Sag is obviously better than that of the northern Lufeng Sag, and it decreases from south to north (Fig. 11(d)). During the sedimentary period of the Upper Wenchang Formation, the porosity of Lufeng 13 Sag and its east, Lufeng 13 Western Sag, and Huizhou 11 Sag and its east and west was relatively large, and the porosity showed an overall trend of decreasing and then increasing from south to north (Fig. 11(c)). The porosity distribution characteristics during the deposition period of Lower Enping Formation show that the perimeter of the sag is larger than its interior, and the area with low porosity is mainly concentrated in the western part of Lufeng 13 East Sag and the center of the northern part of Lufeng Sag (Fig. 11(b)). The Upper Enping Formation has a shallow burial depth and large porosity, which is a continuation of the porosity distribution characteristics of the Lower Enping Formation. The areas with low porosity are concentrated in the southern part of Eastern Lufeng 13 Sag and the central area of northern Lufeng Sag (Fig. 11(a)).

In this study, the potential difference index P_I is used to predict the favorable reservoir area in the Lufeng Sag. When the P_I value of the Enping Formation is less than 0.5, it is a favorable area for effective reservoir development. For the Wenchang Formation, when the P_I value is less than 0.6, it is a favorable area for effective reservoir development. The P_I prediction results show that the effective reservoir favorable areas of the Lower Wenchang Formation are mainly located in the Lufeng 15 Sag, Lufeng 13 Sag, the eastern part of Lufeng 13 West Sag, and the Lufeng 7 Sag and its northern part (Fig. 12(d)). The effective reservoirs of the Upper Wenchang Formation are mainly developed in the Lufeng 13 East Sag and its eastern part, the eastern part of Lufeng 13 Sag, and the Lufeng 7 Sag and its northern part (Fig. 12(c)). The effective reservoirs of the Lower Enping Formation are mainly located

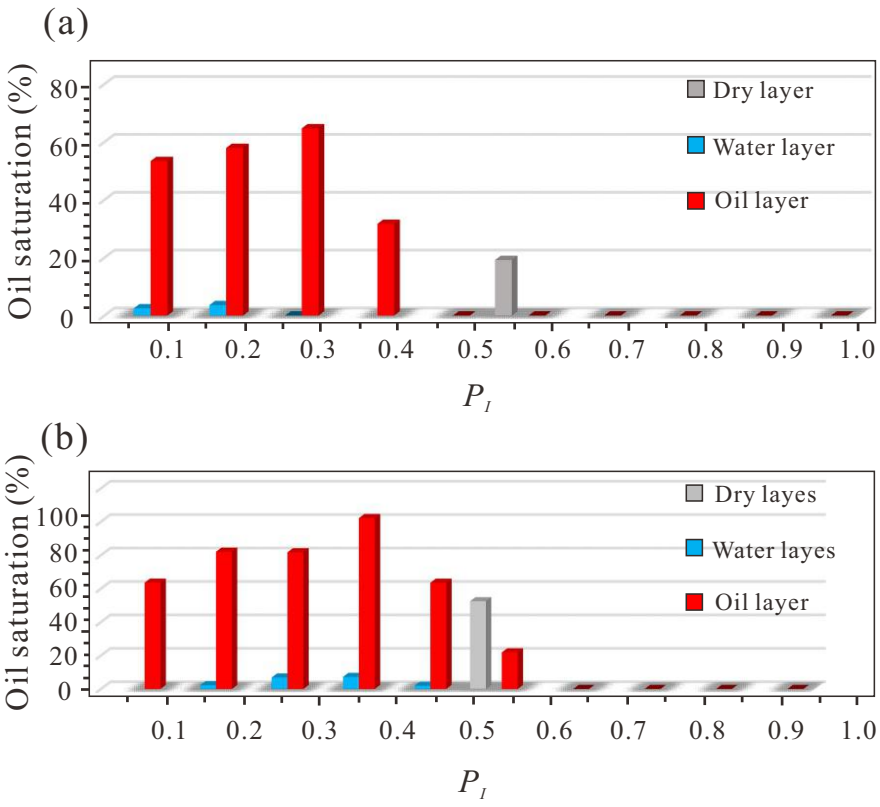

Fig. 10. Relationship between P_I and oil saturation of the (a) Enping Formation (b) and Wenchang Formation in the Lufeng Sag.

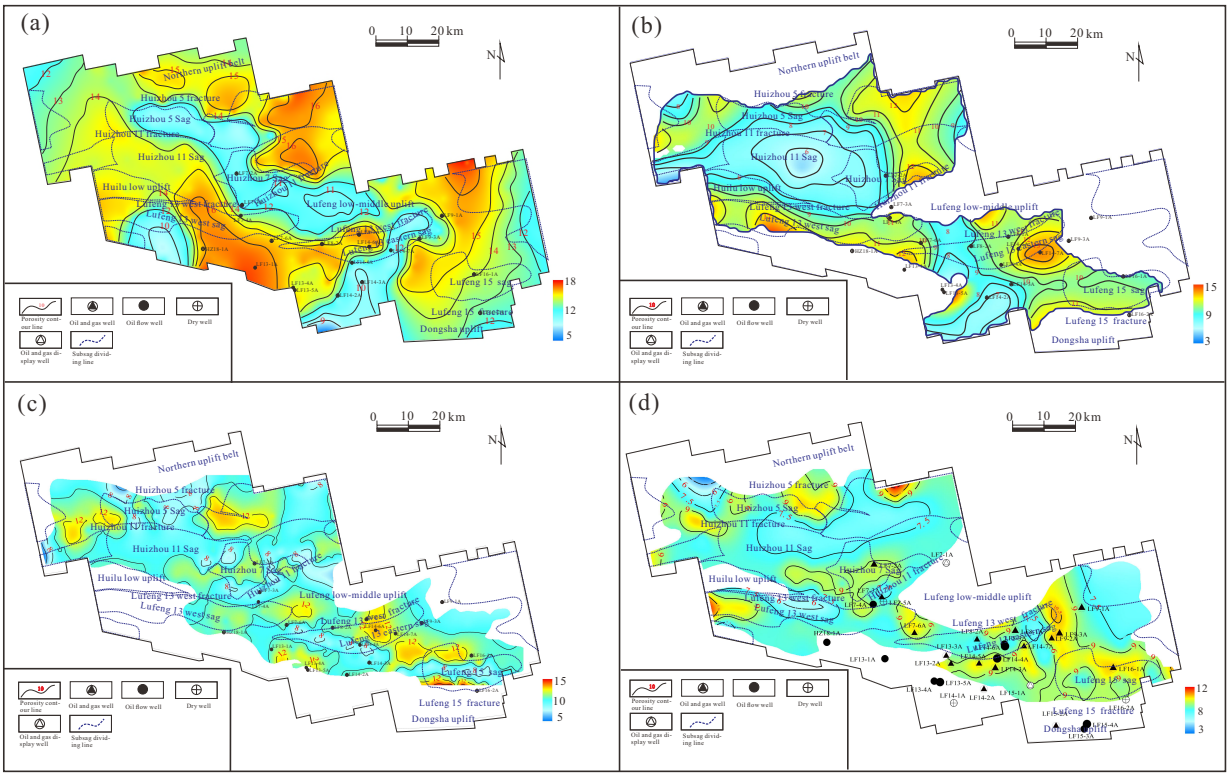

Fig. 11. (a) Porosity distribution of Upper Enping Formation in the Lufeng Sag, (b) Porosity distribution of Lower Enping Formation in the Lufeng Sag, (c) Porosity distribution of Upper Wenchang Formation in the Lufeng Sag and (d) Porosity distribution of Lower Wenchang Formation in the Lufeng Sag.

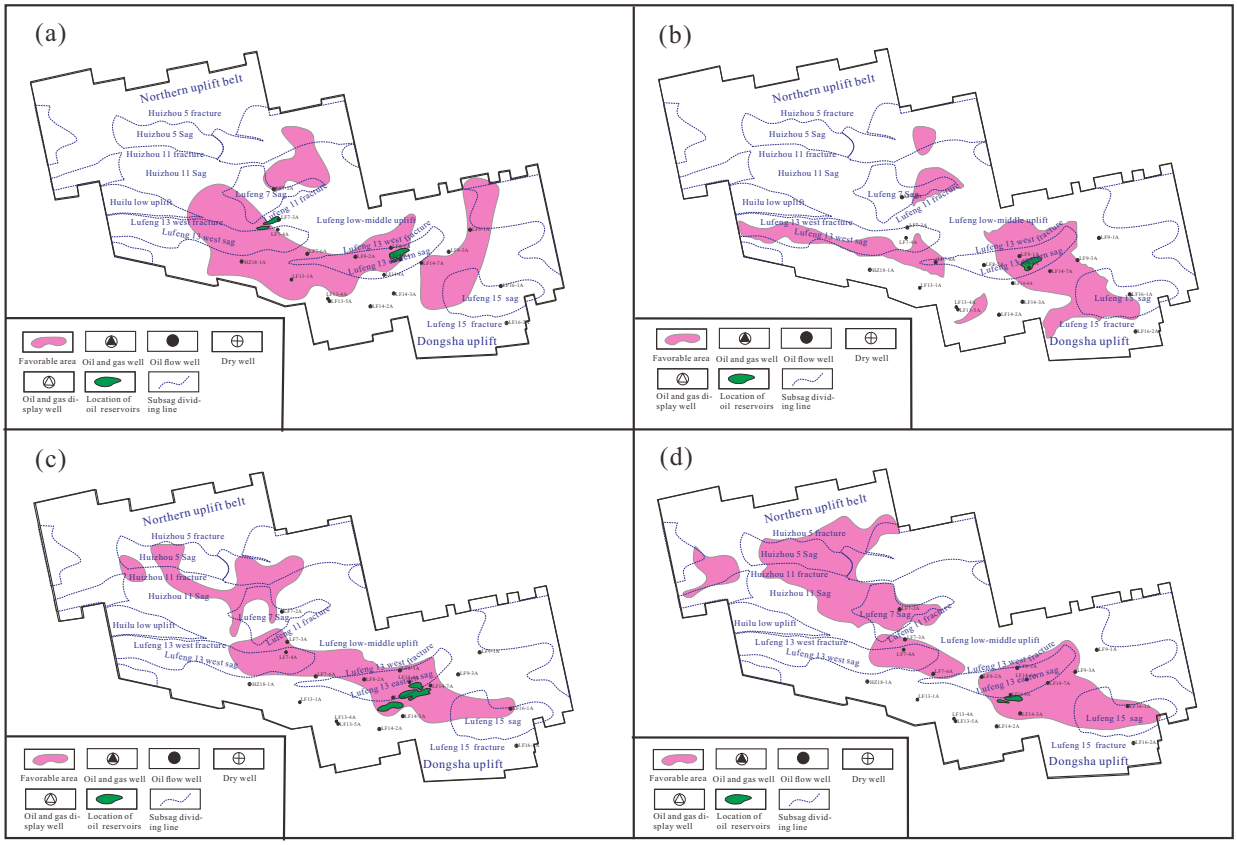

Fig. 12. (a) Favorable reservoir distribution of Upper Enping Formation in the Lufeng Sag, (b) Favorable reservoir distribution of Lower Enping Formation in the Lufeng Sag, (c) Favorable reservoir distribution of Upper Wenchang Formation in the Lufeng Sag and (d) Favorable reservoir distribution of Lower Wenchang Formation in the Lufeng Sag.

in the northeastern part of Lufeng 7 Sag, the Lufeng 13 West Sag and its southern part, the southern part of Lufeng 13 East Sag, and the area of Lufeng 13 East Sag (Fig. 12(b)). The effective reservoir favorable areas of the Upper Enping Formation are mainly located in the western part of Lufeng 13 East sag, the eastern part of Lufeng 13 West Sag, the northern part of Lufeng 7 Sag, and the northern part of Lufeng 15 Sag (Fig. 12(a)). The effective reservoir favorable zone predicted by the potential difference index P_I also has a high degree of agreement with the actual exploration results. It can be found that the currently discovered oil and gas reservoirs are mainly distributed where the potential difference index $P_I < 0.5$, which is basically consistent with the results of the previous conventional evaluation. It can be seen that the prediction of favorable zones for reservoir exploration in the study area by using the potential difference index P_I can provide appropriate guidance for the next step of oil and gas exploration.

4.2 Authenticity check

Here, the sandstone reservoir of the Paleocene Wenchang Formation in well LF14-4A is used as an example to verify the reliability and guiding significance of the proposed method. By calculating the ratio of capillary force between the surrounding rock of each sandstone reservoir and its own capillary force, the effective reservoir in the study area can be distinguished and then compared with the oil bearing conclusion obtained by logging interpretation. The results show that our method presents a good correlation between effective reservoir classification and the oil and gas content of the reservoir interpreted by logging (Fig. 13). At about 21 Ma, there was a phase of hydrocarbon charging in Paleogene reservoirs of the Lufeng Sag. After hydrocarbon generation in the fourth section of Wenchang Formation, hydrocarbon source rocks are transported to the reservoir through sand bodies, fractures and other dominant transport channels, occupying the reservoir pore space. After the oil and gas are injected into the pore space of the reservoir, the damage of pore space caused by compaction and the growth of secondary minerals can be effectively inhibited, such that the reservoir properties can be effectively preserved (Guo et al., 2018). It can be assumed that the capillary force of a reservoir does not change significantly after reservoir formation. However, mudstone becomes dense when buried deep, and the pore throat basically does not change. Therefore, it is considered that the capillary force ratio between the surrounding rock and the reservoir is basically the same at present as that in the reservoir formation period, hence the capillary force ratio that is measured and calculated in the present can be used to approximately replace the capillary force ratio in the reservoir formation period.

Data for the single well LF14-4A show that our method has good correspondence between the effective reservoir iden-

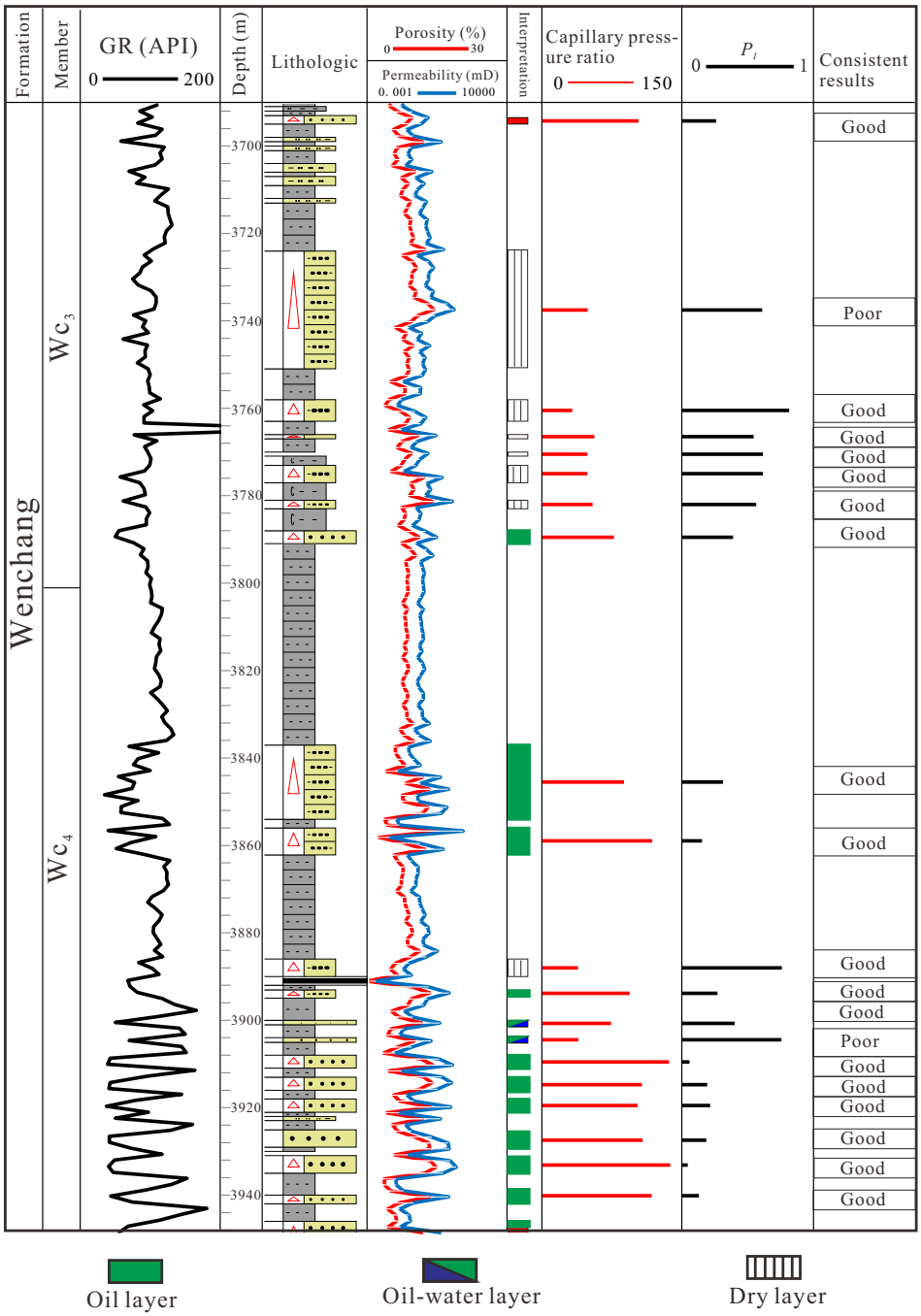

Fig. 13. LF14-4A single well reservoir quantitative evaluation results.

tification results and the reservoir oil and gas properties interpreted by logging. The capillary force difference of the dry layer is smaller, and the corresponding P_I value is larger; on the contrary, the capillary force difference of the oil layer development is larger, and the corresponding P_I value is smaller. The identification degree of effective reservoir is 88.6% consistent with the conclusion of logging interpretation, which indicates that P_I has certain reliability and feasibility in the identification and quantitative evaluation of effective reservoirs.

5. Conclusions

1) Quartz sandstone is the main reservoir rock type in the Lufeng Sag. The pore types are mainly primary pores, and secondary pores are less developed. On the whole, the physical properties of Enping Formation are better than that of Wenchang Formation.
2) The critical capillary force ratio of effective reservoirs increases with the burial depth, which indicates that at the same time, it becomes more difficult to enrich oil and gas. The potential difference index P_I was used to

quantitatively evaluate reservoir quality. The upper limit of P_I index in the Enping Formation was 0.5, and that in the Wenchang Formation was 0.6.

3) Paleogene effective reservoirs in the Lufeng Sag are mainly developed when the P_I is less than 0.5∼0.6. The potential hydrocarbon enrichment target areas are the western area of Lufeng 13 East Sag, the eastern area of Lufeng 13 West Sag and the northeastern area of Lufeng 7 Sag.

Acknowledgements

This study was supported by the Major National R&D Projects of China (No. 2016ZX05024-004) and the research project of CNOOC (Shenzhen) (No. SCKY-2020-SZ-21). We are grateful to CNOOC for providing experimental samples and permitting the publication of this research.

Conflict of interest

The authors declare no competing interest.

References

Athens, N. D., Caers, J. K. A monte carlo-based framework for assessing the value of information and development risk in geothermal exploration. Applied Energy, 2019, 256: 113932.

Barach, B. A. B., Jaafar, M. Z., Gaafar, G. R., et al. Development and identification of petrophysical rock types for effective reservoir characterization: Case study of the Kristine Field, Offshore Sabah. Natural Resources Research, 2021, 30(3): 2497-2511.

Berg, R. R. Capillary pressures in stratigraphic traps. AAPG Bulletin, 1975, 59(6): 939-956.

Ehrenberg, S. N., Nadeau, P. H. Sandstone vs. carbonate petroleum reservoirs: A global perspective on porosity-depth and porosity-permeability relationships. AAPG Bulletin, 2005, 89(4): 435-445.

England, W. A., Mackenzie, A. S., Mann, D. M., et al. The movement and entrapment of petroleum fluids in the subsurface. Journal of the Geological Society, 1987, 144(2): 327-347.

Ge, J., Zhu, X., Zhao, X., et al. Tectono-sedimentary signature of the second rift phase in multiphase rifts: A case study in the Lufeng depression (38-33.9 Ma), Pearl River Mouth Basin, south China sea. Marine and Petroleum Geology, 2020, 114: 104218.

Guo, S., Lu, X., Zhang, Y. Relationship between tight sandstone reservoir Formation and hydrocarbon charging: A case study of a Jurassic reservoir in the eastern Kuqa Depression, Tarim Basin, NW China. Journal of Natural Gas Science and Engineering, 2018, 52: 304-316.

He, H., Li, S., Liu, C., et al. Characteristics and quantitative evaluation of volcanic effective reservoirs: A case study from Junggar Basin, China. Journal of Petroleum Science and Engineering, 2020, 195: 107723.

Huang, H., Li, R., Chen, W., et al. Revisiting movable fluid space in tight fine-grained reservoirs: A case study from Sha-he-jie shale in the Bohai Bay Basin, NE China. Journal of Petroleum Science and Engineering, 2021, 207: 109170.

Huang, Y., Liu, Z., Li, P., et al. Analysis of lithofacies and evaluation of effective reservoirs of member 2 of Xujiahe Formation in the Xinchang area in Western Sichuan. Petroleum Research, 2020, 5(3): 244-253.

Hubbert, M. K. The theory of ground-water motion. The Journal of Geology, 1940, 48(8): 785-944.

Hubbert, M. K. Entrapment of petroleum under hydrodynamic conditions. AAPG Bulletin, 1953, 37(8): 1954-2026.

Huo, Z., Pang, X., Fan, K., et.al. Anatomy and application of facies-potential coupling on hydrocarbon accumulation in typical lithologic reservoirs in Jiyang Depression. Petroleum Geology & Experiment, 2014, 36(5): 574-582. (in Chinese)

Jiang, H., Pang, X., Chen, D., et al. Effective sandstone reservoir determination and quantitative evaluation of deep strata in Kuqa depression, Tarim Basin. Acta Petrol Sinica, 2015, 36(S2): 112-119. (in Chinese)

Jiang, H., Pang, X., Shi, H., et al. Physical threshold of effective reservoir evaluation based on capillary pressure. Geological Review, 2014, 60(4): 869-876. (in Chinese)

Li, Z., Zhang, L., Yuan, W., et al. Logging identification for diagenetic facies of tight sandstone reservoirs: A case study in the Lower Jurassic Ahe Formation, Kuqa Depression of Tarim Basin. Marine and Petroleum Geology, 2022, 139: 105601.

Masters, J. A. Deep basin gas trap western Canada. AAPG Bulletin, 1979, 63(2): 152-181.

Mohaghegh, S. D. Converting detail reservoir simulation models into effective reservoir management tools using SRMs; case study-three green fields in Saudi Arabia. International Journal of Oil, Gas and Coal Technology, 2014, 7(2): 115-131.

Okunuwadje, S. E., MacDonald, D., Bowden, S. Diagenetic and reservoir quality variation of Miocene sandstone reservoir analogues from three basins of southern California, USA. Journal of Earth Science, 2020, 31(5): 930-949.

Pang, X., Chen, D., Zhang, J., et al. Physical simulation experimental study on mechanism for hydrocarbon accumulation controlled by facies-potential-source coupling. Journal of Palaeogeography, 2013, 15(5): 575-592. (in Chinese)

Pang, X., Liu, K., Ma, Z., et al. Dynamic field division of hydrocarbon migration, accumulation and hydrocarbon enrichment rules in sedimentary basins. Acta Geologica Sinica (English Edition), 2012, 86(6): 1559-1592.

Purcell, W. R. Capillary pressures-their measurement using mercury and the calculation of permeability therefrom. Journal of Petroleum Technology, 1949, 1(2): 39-48.

Sun, H., Zhong, D., Zhan, W., et al. Reservoir characteristics in the Cretaceous volcanic rocks of Songliao Basin, China: A case of dynamics and evolution of the volcano-

porosity and diagenesis. Energy Exploration & Exploitation, 2019, 37(2): 607-625.

Tang, P., Chen, D., Wang, Y., et al. Diagenesis of microbialite-dominated carbonates in the Upper Ediacaran Qigebrak Formation, NW Tarim Basin, China: Implications for reservoir development. Marine and Petroleum Geology, 2022, 136: 105476.

Tian, L. Genesis mechanism of tuffaceous materials in Paleogene Large-scale glutenite reservoirs and implications for hydrocarbon exploration in the Huizhou Depression, Pearl River Mouth Basin. Earth Science, 2022, 47(2): 452-463. (in Chinese)

Wang, C., Chen, D., Li, H., et al. Differential genetic mechanisms of deep high-quality reservoirs in the Paleogene Wenchang Formation in the Zhu-1 depression, Pearl River Mouth Basin. Energies, 2022, 15(9): 3277.

Wang, W., Pang, X., Chen, Z., et al. Improved methods for determining effective sandstone reservoirs and evaluating hydrocarbon enrichment in petroliferous basins. Applied Energy, 2020, 261: 114457.

Wang, T., Pang, X., Max, I., et al. The genetic mechanism and model of deep-basin gas accumulation and methods for predicting the favorable areas. Acta Geologica Sinica (English Edition), 2003, 77(4): 547-556.

Wang, D., Xin, B., Yang, H., et.al. Zircon SHRIMP U-Pb age and geological implications of tuff at the bottom of Chang-7 Member of Yanchang Formation in the Ordos Basin. Science China Earth Sciences, 2014, 57(12): 2966-2977.

Wang, X., Zhang, X., Lin, H., et al. Paleogene geological framework and tectonic evolution of the central anticlinal zone in Lufeng 13 sag, Pearl River Mouth Basin. Petroleum Research, 2019, 4(3): 238-249.

Wu, W., Li, Q., Pei, J., et al. Seismic sedimentology, facies analyses, and high-quality reservoir predictions in fan deltas: A case study of the Triassic Baikouquan Formation on the western slope of the Mahu Sag in China's Junggar Basin. Marine and Petroleum Geology, 2020, 120: 104546.

Zeng, Q., Mo, T., Zhao, J., et al. Characteristics, genetic mechanism and oil & gas exploration significance of high-quality sandstone reservoirs deeper than 7000 m: A case study of the Bashijiqike Formation of Lower Cretaceous in the Kuqa depression, NW China. Natural Gas Industry B, 2020, 7(4): 317-327.

Zhou, J., Qiao, X., Wang, R., et al. Effective reservoir development model of tight sandstone gas in Shanxi Formation of Yan'an Gas Field, Ordos Basin, China. Journal of Natural Gas Geoscience, 2022, 7(2): 73-84.

Zhu, M., Liu, Z., Liu, H., et al. Structural division of granite weathering crusts and effective reservoir evaluation in the western segment of the northern belt of Dongying Sag, Bohai Bay Basin, NE China. Marine and Petroleum Geology, 2020, 121: 104612.